CREATING HIGH-DENSITY LARGE SQUARE BALES BY RECOMPRESSION

J. R. McAfee, K. J. Shinners, J. F. Friede, C. P. Walters

ABSTRACT. *Creating high-density biomass bales would reduce the number of bales handled, stored, and transported to biorefineries, thereby reducing costs. Recompression of large square bales is one approach to increase bale density; however, recompression research on large bales is limited. Recompression of common biomass crops in 80 cm × 90 cm nominal cross-section bales was used to quantify pressure-density and stress relaxation relationships as well as restraining forces required to maintain compressed densities. Linear, power, and exponential models were fit to the pressure-density data, with the linear model providing the best representation of the recompression process. When bales were recompressed soon after bale formation, density increased by an average of 134%, and the target dry-basis density of 205 kg m^{-3} was exceeded at the end of recompression with all crops. While still compressed, bales were wrapped with four steel cables configured with load cells to measure the restraining force after release of pressure followed by bale re-expansion. Total restraining forces ranged from 18 to 40 kN. Bale density decreased by an average of 17% due to re-expansion after pressure was released. Strain relief induced by allowing the bale to re-expand by approximately 10% before placing the cables around the bales reduced the required restraining force by an average of 35%. Although the forces applied were great (>560 kN), the dry-basis specific energy requirements were comparatively low (0.18 to 0.29 kWh Mg^{-1}) because recompression took place over a relatively long duration of approximately 20 to 25 s. Recompressing large square bales is a low-energy method to achieve bale densities that should ensure weight-limited biomass transport.*

Keywords. *Bales, Biomass, Compression, Energy.*

The large square bale (LSBe) is currently the most common biomass feedstock package, primarily because it produces the greatest package density (Shinners and Friede, 2018). Bale density has been identified as having the greatest influence on feedstock costs because it impacts the number of packages to be aggregated, handled, stored, and transported (Kenney et al., 2014; Shah and Darr, 2016). To achieve legal transport weight limits, the LSBe density should be approximately 240 kg m^{-3} on a wet basis (Miao et al., 2013). If the bale moisture is assumed to be 15% (w.b.), then the target dry-basis density would be 205 kg m^{-3}. Using conventional balers, LSBe dry-basis densities of only 145 to 200 kg m^{-3} have been reported for various biomass crops (Kemmerer and Liu, 2014; Shinners et al., 2007, 2010; Shinners and Friede, 2018). To produce high-density (HD) bales, manufacturers have modified large square balers (LSBrs) to produce greater pressure on the bale face by increasing the resistance to bale movement through the open bale chamber. This is typically accomplished by using a longer bale chamber and increasing the bale chamber convergence. Although greater compression forces are achieved, these forces are repeatedly applied and then released as the plunger reciprocates at relatively high frequencies. This method of compression yields maximum compressive forces only for a fraction of a second and allows a considerable amount of elastic rebound as the plunger retracts. The elastic rebound experienced by each flake increases the total energy demand of densifying the entire bale, so densification by this method is inefficient. Greater plunger forces require more robust drive components and frames, so baler costs increase. Although greater density can be achieved, increased harvest costs due to the more expensive baler, the larger tractor required, and higher operating costs (fuel, stronger twine, etc.) may overwhelm the cost savings in storage and transport (Sokhansanj et al., 2014). Bale densities in excess of the target of 205 kg m^{-3} were achieved with a HD LSBr; however, the specific energy requirements increased exponentially with bale density (Shinners and Friede, 2018). Bale recompression after formation of low-density bales is potentially a more economical method of achieving the target bale density.

Recompression of LSBes has been used for densification of high-value hay crops intended for export. Recompression normally takes place at capital-intensive industrial-scale facilities where large hydraulic presses can produce alfalfa bales with density up to 480 kg m^{-3} (Steffen Systems, 2018). Recompression to these densities can only be economically justified for high-value forages to be shipped long distances in overseas containers because the cost of recompression can

Submitted for review in April 2018 as manuscript number MS 12898; approved for publication by the Machinery Systems Community of ASABE in January 2019.

The authors are **Joshua R. McAfee,** former Graduate Research Assistant, **Kevin J. Shinners,** Professor, **Joshua F. Friede,** Associate Instrumentation Specialist, and **Chase P. Walters,** former Graduate Research Assistant, Department of Biological Systems Engineering, University of Wisconsin, Madison, Wisconsin. **Corresponding author:** Kevin J. Shinners, 460 Henry Mall, University of Wisconsin, Madison, WI 53706; phone: 608-263-0756; e-mail: kjshinne@wisc.edu.

  ISSN 2151-0032 https://doi.org/10.13031/trans.12898

exceed \$30 Mg^{-1} (Brownell and Liu, 2011). Although economically viable for high-quality animal feed, the industrial-scale off-farm recompression process may not be economically viable for biomass feedstocks. What is required is a more economical means of recompressing biomass bales in the field to dry-basis densities up to 205 kg m^{-3}. In-field densification allows the cost benefits of greater density to be realized throughout the supply chain (i.e., aggregation, storage, handling, and transport).

Much of the previous research on compression of hay and biomass materials has focused on small laboratory fixtures used to compress loose materials to high-density cubes, wafers, or pellets (O'Dogherty and Wheeler, 1984; O'Dogherty, 1989; Van Pelt, 2003). Limited research has been conducted on recompressing small square bales (Talebi et al., 2011; Wang and Liu, 2014), and it is unknown if these results can be scaled to LSBes. Therefore, research is needed to quantify the recompression properties of LSBes.

What is proposed here is in-field recompression of LSBes in which low-cost conventional baler mechanisms would form the bale shape and deliver the low-density bale to a recompression system integrated with the baler. Densification by recompression and then restraint of the bale would occur during the 30 to 60 s while the next bale is formed. Although densification forces are large, these forces can be applied over a relatively long duration so that specific energy requirements are potentially much less compared to those required by current HD LSBrs. Current tractors likely have adequate hydraulic flow and pressure to produce the needed forces with reasonable size-compression cylinders. After densification, there may be sufficient dwell time available for material stress relaxation, allowing the material to lose some of its resiliency before the bale is restrained, thereby reducing recoil forces, maintaining the achieved density, and allowing the use of lower-cost restraining material (Watts and Bilanski, 1991). To develop such a system, an understanding of recompression properties of LSBes of biomass is required, so the objectives of this research were: (1) to quantify pressure-density and stress relaxation relationships while recompressing LSBes, and (2) to measure the restraining forces required to maintain the achieved densities.

MATERIALS AND METHODS

The test fixture had a rectangular prism compression chamber with a plunger at one end and a door at the other (McAfee, 2018). The chamber had a constant cross-section of 90 cm × 90 cm and a length of 2.1 m. Bales were loaded through the rear door, and the closed and locked door produced the main resisting force to the compression force applied by the plunger. The plunger was supported by eight bearings riding on two rails, and it was actuated by a double-acting cylinder with a 184 mm cap end bore, 115 mm rod diameter, and 2.0 m stroke. A John Deere 8R Series tractor was used to power the cylinder through a closed-center hydraulic system at pressures up to 200 bar so that the plunger could apply over 700 kPa to the bale face. Hydraulic flow rate was set so that recompression took place in approximately 20 to 25 s. This duration was chosen because it equals approximately half the time required to make a LSBe in a conventional LSBer. After compression and restraint, the rear door was opened and bales were ejected by the plunger. Parasitic forces due to internal cylinder and plunger bearing friction were measured while operating the apparatus without compressing a bale and at approximately the average linear velocity (45 mm s^{-1}) used during bale compression. The parasitic forces (1.4 kN) were then subtracted from the force measurement (eq. 1).

To determine cylinder forces, pressure transducers (PX305-7.5KGI and PX305-3KGI, Omega Engineering, Stamford, Conn.) were placed in ports plumbed directly into the cap and rod ends of the cylinder, respectively, so that they measured the cylinder internal pressures. A string potentiometer (SR1V-125, Celesco Transducer Products, Toronto, Canada) was used to measure the linear displacement of the plunger. All the sensors were excited at 15 V with a power supply (EYE-600W-15V-40, Eyeboot, Hong Kong, China), and data were recorded at 5 Hz using a datalogger (model 21X, Campbell Scientific, Logan, Utah). Bale face pressure was determined by:

$$P = \frac{F_{plunger}}{A_{bale}} = \frac{\left(P_{ce} \cdot A_{ce}\right) - \left(P_{re} \cdot A_{re}\right) - F_f}{A_{bale}} \quad (1)$$

where the applied bale face pressure P (kPa) was a function of applied plunger force ($F_{plunger}$), the cap and rod end cylinder pressures (P_{ce} and P_{re}, respectively), the cap and rod end areas (A_{ce} and A_{re}, respectively), friction forces (F_f), and the cross-section of the bale (A_{bale}, typically 0.81 m^2).

After bales were loaded into the chamber, the twines were cut to allow the bale to expand laterally to the full extent of the chamber, and the instrumentation and hydraulic systems were then initiated to begin recompression of the bale. Recompression continued until the maximum pressure of the tractor's hydraulic system was reached, and then plunger displacement stopped. The tractor's selective control valve (SCV) was then placed in neutral, which trapped the oil in the cylinder. To quantify force relaxation, cylinder hydraulic pressure was measured for 60 s after compression in the 2016 tests and for the entire duration (approx. 5 min) required to apply the restraining cables in the 2017 tests. Four 6 mm diameter steel cables (6.2 kN working limit) were then placed around the recompressed bale in the original location of the twines. The cables were fabricated with a loop at each end, and one loop was connected to several links of chain. A chain "quick link" was used to join the two ends of the cable together and form a closed loop around the bale. Efforts were made to select the chain link connection point that minimized slack in the cables, and all cables were made the same length. With the cables in place, two-point bending load cells were then placed in parallel with each cable. The clamp-on load cells (model DLWS-1t, Load Cell Central, Milan, Pa.) had 9.8 kN capacity. Calibration relationships between cable tension and load cell output had been previously determined (McAfee, 2018) using a universal tension tester (MTS Insight, MTS Systems Corp., Eden Prairie, Minn.). While the

cables were applied, data collection from the recompression cylinder continued so that bale relaxation properties could be determined. A datalogger (model 21X, Campbell Scientific) was used to excite the cable load cells and then record the load cell output at 5 Hz. Typically, approximately 5 min was needed to apply the cables and load cells. To allow the compressed bale to expand, the plunger was retracted by the tractor's hydraulic system, and the chamber door was opened. The bale was then allowed to sit with the cables restraining the material for an additional 60 s. The total restraining force of the cables was calculated as the sum of the final force measured by the four load cells multiplied by 2. Although friction with the recompression chamber contributed to restraining the bale expansion, this contribution could not be accounted for.

A second test procedure was developed to quantify the relationship between applied force and bale density during the short duration between when the plunger load was removed and the cables fully restrained the bale. The recompression system's hydraulic circuit was modified to allow controlled flow of oil from the cylinder as the bale expanded (McAfee, 2018). A needle flow-control valve was used to limit flow from the compression cylinder so that re-expansion took place over approximately 5 s. After the cables and load cells were in place, the tractor's SCV was moved to the float position so that bale expansion forced the plunger to begin retraction. The bale was allowed to expand in this controlled manner until the cables were the principal means of restraining the bale. The cylinder instrumentation system remained active from initial recompression, through bale relaxation (i.e., cable attachment), and finally during controlled bale expansion. After the cables became taut and the plunger movement caused by bale re-expansion had stopped, the plunger was retracted by the tractor's hydraulic system and the cable restraint procedure was then similar to that of the first test procedure.

A final test procedure was used to determine the beneficial aspects of relieving some bale strain prior to applying the cable restraints. After recompression stopped, the plunger remained at rest for approximately 5 s to allow some stress relaxation of the biomass material under constant strain. The bale was then allowed to re-expand to reduce strain by approximately 10% (i.e., compressed length increased by 10%) by placing the tractor's SCV in the float position. After the bale had expanded by 10%, the tractor's SCV was placed into neutral, and then all other aspects of the test procedure were identical to the second test procedure described above.

Bales were created with a Case IH model LB 334 baler to a target length of 2.0 m. Initial dry-basis bale density ranged from 106 to 194 kg m^{-3} (table 1). Six replicate bales were compressed except in cases when material availability was limited. In initial tests using the first test procedure, bales had been in storage for several months before they were recompressed, while later tests using the second and third test procedures were conducted within a few days of baling. In either case, some degree of rheological relaxation certainly occurred before recompression. Alfalfa and fescue bales were from a second crop harvested in July. Reed canarygrass and switchgrass bales were harvested in early October after senescence and a killing frost. Wheat straw and corn stover were harvested in August and November, respectively, shortly after grain harvest. Bales were chosen at random based on subjective assessment of uniformity and appropriate length to fit into the chamber.

After bales were removed from the recompression chamber, they were weighed using an 1800 kg capacity platform scale with a resolution of 0.5 kg. Each bale was subsampled in two locations for moisture determination using a 5 cm diameter by 80 cm long boring tool. All moisture bore samples were then oven-dried for 24 h at 103°C according to ASABE Standard S358.2 (ASABE, 2012). The plunger potentiometer data were used to quantify bale length for volume determination while the bale was in the test fixture. The bale volume after it had been removed from the fixture was determined by measuring relevant bale dimensions to the nearest 2 cm at several locations and averaging these measurements. Typical bale cross-section was 0.81 m^2.

MODEL ANALYSIS

Compressing loose biological materials is considered a two-stage process. The first stage of the process is dominated by consolidation and void reduction (Faborode and O'Callaghan, 1989). The second stage is defined by the elastic and plastic deformation of stem structures as the material is further compressed (O'Dogherty, 1989). As compression transitions from consolidation and void reduction to deformation, increased pressure results in small incremental increases in density. If compression does not permanently crush or deform the stems, then the material will elastically rebound and expand upon the release of applied pressure, reducing bale density (Mohsenin, 1970).

Models have previously been suggested to describe the

Table 1. Bale properties and number of replicate bales tested using three rest procedures.

	First Test Procedure[a]					Second Test Procedure[b]					Third Test Procedure[c]				
		Moisture (% w.b.)		Density[d] (kg m^{-3})			Moisture (% w.b.)		Density[d] (kg m^{-3})			Moisture (% w.b.)		Density[d] (kg m^{-3})	
Crop	No. of Bales	Avg	SE	Avg	SE	No. of Bales	Avg	SE	Avg	SE	No. of Bales	Avg	SE	Avg	SE
Alfalfa	6	14.4	0.3	194	1	6	15.4	0.3	179	4	-	-	-	-	-
Corn stover	12	18.8	0.4	140	6	6	25.9	1.3	111	3	4	25.2	2.5	113	3
Fescue	6	15.3	0.1	163	2	6	13.9	0.2	143	3	-	-	-	-	-
Reed canarygrass	-	-	-	-	-	6	11.4	0.2	144	5	3	13.8	1.2	141	7
Switchgrass	6	14.7	0.1	122	4	6	13.2	0.3	132	1	3	12.8	0.4	134	1
Wheat straw	6	11.1	0.3	112	2	6	9.4	0.8	108	3	6	8.7	0.1	106	3

[a] Compression, relaxation, and restraint properties measured.
[b] Compression, relaxation, controlled expansion, and restraint properties measured.
[c] Identical to second test procedure except that bales were allowed to re-expand 10% before restraining cables attached.
[d] Initial dry-basis density of bales prior to recompression.

compression of loose biomass material, with the power function being the most common (O'Dogherty and Wheeler, 1984):

$$\rho = k \cdot P^{n} \tag{2}$$

where the instantaneous bale density ρ (kg m^{-3}) is a function of applied pressure P (kPa) raised to a rate coefficient (n) and then multiplied by the initial density coefficient (k).

An exponential model suggested by Faborode and O'Callaghan (1989) expressed density as:

$$\rho = \left(\frac{\rho_o}{B}\right) \ln\left(\frac{P \cdot B}{A \cdot \rho_o} + 1\right) \tag{3}$$

where P is the applied pressure (kPa), ρ_o is the initial density (kg m^{-3}), ρ is the instantaneous density (kg m^{-3}), A is the incompressibility, and B is the porosity index.

When bales are recompressed, much of the consolidation and void reduction has already taken place in the baler, so the power and exponential models may underpredict the initial and final density of partially compressed bales (Lacy and Shinners, 2016). A simple linear function could be used to predict the density of the re-compression process:

$$\rho = (m \cdot P) + I \tag{4}$$

where ρ is the instantaneous bale density (kg m^{-3}), P is the pressure applied (kPa), m is the rate of densification, and I is the initial bale density (kg m^{-3}).

When the pressure on the bale face is maintained and strain is constant, the bale exhibits stress relaxation behavior. Peleg (1980) suggested that the stress relaxation relationship of biological materials with time can be normalized and presented in a linear form:

$$F(t) = F_i - \left(\frac{F_i \cdot t}{(k_1 + k_2 \cdot t)}\right) \tag{5}$$

where $F(t)$ is the decaying force (kN), F_i is the initial force (kN), t is the elapsed time (s), and k_1 and k_2 are coefficients to model the plunger force during constant-strain stress relaxation.

A relationship similar to equation 5 was used to model the plunger force during controlled bale expansion when the plunger was moved by the expanding bale and the cables became taut to begin restraining the bale. This model relates the force applied to the bale by the plunger (stress) as a function of the change in bale density (strain) with expansion:

$$F(\rho) = F_i - \left(\frac{F_i \cdot \Delta\rho}{(k_3 + k_4 \cdot \Delta\rho)}\right) \tag{6}$$

$$\Delta\rho = \rho - \rho_{rc} \tag{7}$$

where Δρ is the change in bale density during re-expansion (kg m^{-3}), ρ is the instantaneous density (kg m^{-3}), ρ_{rc} is the recompressed density (kg m^{-3}), F_i is the force applied to the plunger by the bale at the end of the constant-strain relaxation period (kN), $F(\rho)$ is the instantaneous force the bale exerts on the plunger as the bale expands into the restraining cables (kN), and k_3 and k_4 are model coefficients.

Regression analysis using Excel's Solver data analysis package was used to find the pressure-density (eqs. 2 through 4), relaxation (eq. 5), and controlled expansion (eq. 6) model coefficients for each individual bale by iteratively minimizing the sum of squares of the differences between the actual and model data. The individual bale model coefficients were then used to predict bale density or plunger force by interpolating through a representative range of pressures (pressure-density models), time (relaxation model), or bale densities (plunger force) using either the Fit *X* by *Y* (linear model) or Nonlinear Modeling (power and exponential recompression, relaxation, or controlled expansion models) tools in JMP Pro (ver. 13.1, SAS Institute Inc., Cary, N.C.). These JMP tools also provided an analysis of uncertainty that provided a 95% confidence interval for the interpolated model coefficients. The JMP tools were also used generate least significant differences (LSD) at 5% significance level so that significant differences in bale density, plunger force, cable restraint force, or energy requirements between crops could be determined.

Results and Discussion

Recompression

During compression, bales were observed to expand and fill the cross-section of the bale chamber. After restraint and removal from the chamber, the measured bale width and height were typically slightly less than the bale chamber (90 cm × 90 cm). Excluding alfalfa, the overall average dry-basis bale density prior to recompression for the remaining crops was 128 kg m^{-3} (table 1), considerably below the target density of 205 kg m^{-3}. The final recompressed dry-basis density exceeded this target for all crops (table 2). Alfalfa had the greatest pre- and post-compressed density, and wheat straw had the least. The difference in initial densities between crops was one of several contributing factors that explain the observed differences in final density between crops.

Pressure-density relationships for recompression did not exhibit the typical two-stage process of loose material because considerable void reduction and consolidation had already occurred during baling. Although some additional void reduction certainly occurred during recompression, this process was likely dominated by elastic and plastic stem deformation, so the pressure-density relationships often appeared linear (fig. 1). The power function is well suited to model the pressure-density relationship for the two-phase compression of loose material (O'Dogherty, 1989), but it did not do well in predicting the density of recompressed bales (Lacy and Shinners, 2016; McAfee, 2018). The power function consistently underpredicted the initial and final compressed densities, and therefore this function was not considered further. The slope (m) for the linear model (eq. 4) described the rate of increase of the pressure-density function. The rate of increase for the exponential model (eq. 3) was controlled by both the incompressibility (A) and the porosity index (B) parameters.

Table 2. Average recompression model coefficients, 95% confidence intervals (CI) for interpolated model coefficients, and predicted dry-basis bale density for the linear and exponential models (eqs. 3 and 4).

Test Procedure and Crop	Pressure-Density Model Coefficients				Maximum Compressed Bale Density (kg m^{-3})			
	Linear[a]		Exponential[b]		Measured		Predicted[c]	
	m ±CI	*I* ±CI	*A* ±CI	*B* ±CI	Avg	SE	Linear	Exponential
2016[d]								
Alfalfa	0.24 ±0.01	192.5 ±6.7	2.97 ±0.47	0.62 ±0.37	373 a	11	371 a	377 a
Corn stover	0.19 ±0.02	129.5 ±6.9	5.28 ±1.09	0.0053 ±0.41	278 b	12	273 c	280 c
Fescue	0.16 ±0.01	165.4 ±2.8	3.53 ±0.66	1.2 ±0.37	286 b	5	284 bc	291 bc
Switchgrass	0.25 ±0.02	135.1 ±11.1	1.79 ±0.79	0.78 ±0.04	318 b	18	317 b	323 b
Wheat straw	0.16 ±0.01	113.1 ±2.9	4.04 ±1.07	0.44 ±0.44	208 c	11	210 d	207 d
LSD[e] (p = 0.05)					44		38	33
2017[f]								
Alfalfa	0.26 ±0.01	177.7 ±5.5	2.61 ±0.56	0.67 ±0.33	368 a	10	365 a	370 a
Corn stover	0.27 ±0.01	115.0 ±3.5	2.71 ±0.36	0.33 ±0.12	314 b	11	308 bc	309 c
Fescue	0.29 ±0.01	157.4 ±4.2	1.24 ±0.31	1.1 ±0.18	361 a	5	367 a	364 a
Reed canarygrass	0.23 ±0.01	154.1 ±2.6	1.92 ±0.28	1.0 ±0.14	322 b	4	323 b	325 b
Switchgrass	0.20 ±0.00	143.0 ±1.6	2.14 ±0.22	1.1 ±0.10	295 c	4	294 c	297 c
Wheat straw	0.17 ±0.01	116.9 ±2.3	2.23 ±0.43	1.3 ±0.18	237 d	7	238 d	238 d
LSD[e] (p = 0.05)					15		20	14

[a] Linear model coefficients (eq. 4) determined by regression of interpolated individual bale data.
[b] Exponential model coefficients (eq. 3) determined by regression of interpolated individual bale data.
[c] Dry-basis density predicted by using indicated model and interpolated model coefficients.
[d] Recompression data collected during tests using the first test procedure (table 1).
[e] Least square difference. Averages in columns with different letters are significantly different at 5% significance level.
[f] Recompression data collected during tests using the second and third test procedures (table 1).

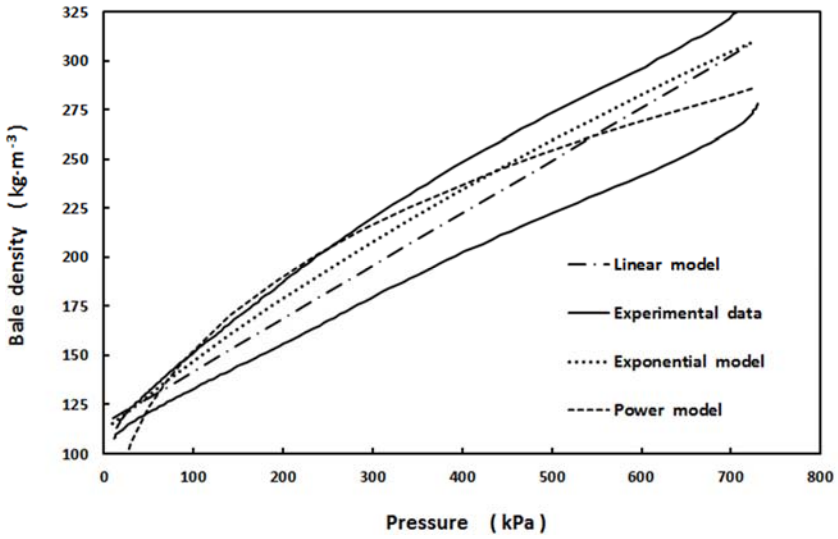

Figure 1. Power, exponential, and linear models (eqs. 2 to 4) to predict dry-basis bale density based on applied pressure using interpolated model coefficients (table 2). Experimental data represent the maximum and minimum densities achieved with corn stover bales in 2017.

Using the interpolated model coefficients, the error in predicted final dry-basis density for the both the linear and exponential models was 1.3% (table 2). Model coefficients and initial and final densities varied for the same crop type between 2016 and 2017 (table 2). Although the model coefficients were different between years, the predicted pressure to achieve a given density using these different coefficients was similar between years for alfalfa, switchgrass, and wheat straw, but not for corn stover or fescue. Corn stover baled in 2017 had greater moisture than desired (table 1), which may have contributed to differences in achieved density. In 2017, fescue had much smaller stem diameters than bales compressed in 2016, which may have contributed to differences in achieved density between years. Uncontrolled factors, such as the timing of harvest and the duration of time the bales were in storage (months in 2016 and days in 2017), could have also affected recompression properties between the two years.

Bale recompression behavior is affected by physical properties, such as leaf:stem ratio, lignin content, friction coefficient, stem stiffness (modulus of elasticity), and stem bending strength (Kemmerer and Liu, 2014). Materials with greater friction coefficients have more resistance to particles sliding over one another and increase the force required for recompression. Stiffer materials are more difficult to compress and require more pressure to reach a given density. Stems with greater bending strength require more force to reshape in the compression chamber. Fine-stem, leafy crops such as alfalfa and fescue (2017) were compressed to the target density with less force than any of the other crops (fig. 2). Reed canarygrass and switchgrass have heavy, brittle stems that required more pressure to compress than the fine-stem

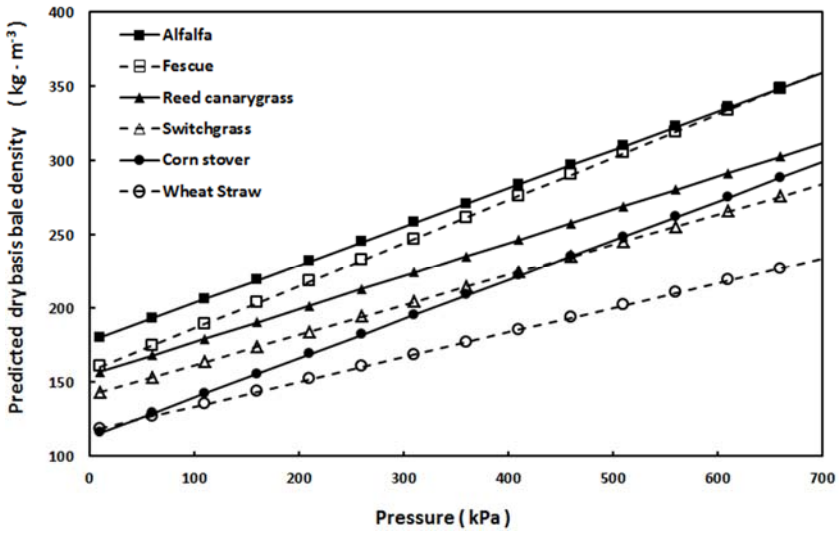

Figure 2. Predicted dry-basis bale density for a given applied pressure for recompressed bales using the interpolated linear model coefficients (eq. 4 and table 2).

crops. Wheat straw has large, hollow stems that are difficult to plastically deform (O'Dogherty et al., 1995), so this crop required the greatest pressure to achieve a given density.

The specific energy required for recompressing LSBes was determined by numerical integration of the force-displacement data obtained during recompression. Corn stover required the greatest energy, while the fine-stem crops (alfalfa and fescue) required the least energy (table 3). With the exception of wheat straw, specific energy was similar between years for the same crop. Wheat straw was compressed to greater density in 2017, which was a contributing factor for the greater energy required. Dry-basis specific energy across both years and all crops ranged from 0.175 to 0.291 kWh Mg^{-1} (table 3). The rate of recompression was approximately 45 mm s^{-1}, similar to that used by Hofstetter and Lui (2011) for recompressing small square bales and by Lacy and Shinners (2016) for recompressing large round bales, and the range of energy required for recompressing LSBes was similar to that reported for these other bale types. The power required for recompressing LSBes was relatively low because densification occurred over a relatively long duration (20 to 25 s in this research). During approximately the first 10 s of compression, the required hydraulic power was typically less than 4 kW. Power then typically increased linearly for approximately 7 s. The peak power at the end of this period was typically 20 to 25 kW. As the hydraulic pressure approached maximum (approx. 200 bar), the tractor's load-sensing hydraulic system gradually destroked the pump toward zero flow, so hydraulic power decreased linearly during final compression. For comparison, the compression process in a LSBr typically occurs in less than 0.5 s. The dry-basis specific energy required to create bales at 147 and 209 kg m^{-3} with a HD LSBr was 2.71 and 3.74 kWh Mg^{-1}, respectively (Shinners and Friede, 2018), which means that a 62 kg m^{-3} increase in bale density required an additional 1.03 kWh Mg^{-1}. Recompression achieved a larger improvement in density but required less than 30% of the specific energy required by a conventional HD plungerhead LSBr. Recompression duration could be varied with an in-field recompression device depending on crop type, desired productivity, and desired density. Any change in the recompression rate would be accompanied by a corresponding change in the specific energy required to reach a given densification level. Should this process be integrated into a baler, the short duration of maximum required hydraulic power can be well managed by the tractor's engine governor and fuel control system.

Table 3. Specific energy requirements (dry basis) for recompression based on numerical integration of the force-displacement data.

	Specific Energy (kWh Mg^{-1})			
	2016[a]		2017[b]	
Crop	Avg	SE	Avg	SE
Alfalfa	0.175 b	0.003	0.181 d	0.004
Corn stover	0.291 a	0.012	0.278 a	0.011
Fescue	0.185 b	0.002	0.204 c	0.019
Reed canarygrass			0.209 c	0.007
Switchgrass	0.251 ab	0.008	0.228 b	0.003
Wheat straw	0.223 b	0.035	0.277 a	0.005
LSD[c] (p = 0.05)	0.056		0.017	

[a] Recompression data collected using first test procedure (table 1).
[b] Recompression data collected using second and third test procedures (table 1).
[c] Least square difference. Averages in columns with different letters are significantly different at 5% significance level.

Relaxation and Restraining Force

While the restraining cables were applied and the bale was held under fixed displacement (i.e., constant strain), the plunger force decreased as the compressed material underwent stress relaxation (fig. 3). Similar stress relaxation of compressed hay and biomass material has been reported (Watts and Bilanski, 1991; Juan et al., 2010; Talebi et al., 2011). The plunger force decreased by an average of 29% or 36% when relaxation occurred over an average duration of 50 or 280 s using the first and second test procedures, respectively (table 4). The interpolated relaxation coefficients (eq. 5) were used to predict the reduction in plunger force for all crops compressed in 2017. Stress relaxation was estimated to reduce the plunger force by 8%, 16%, and 41% after arbitrary constant strain durations of 7, 20, and 100 s, respectively. There were differences in the stress relaxation model coefficients for

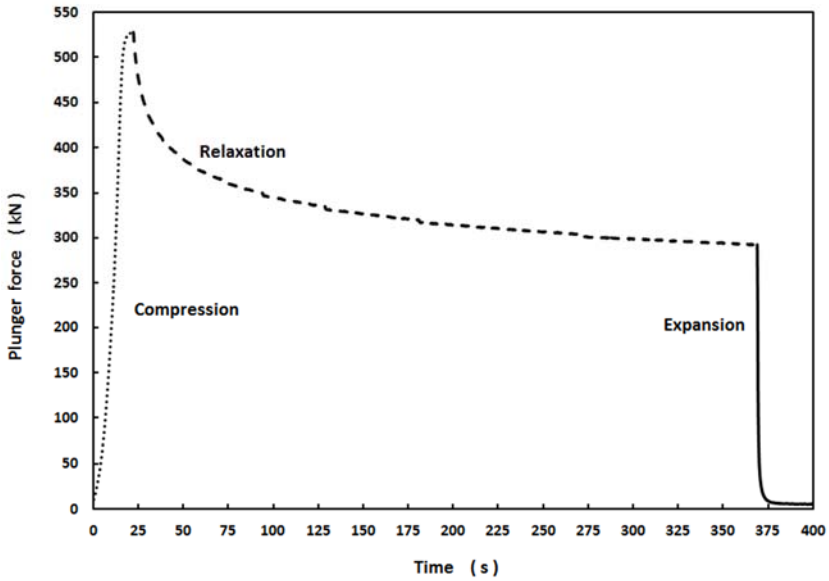

Figure 3. Plunger force versus time during compression, stress-relaxation during constant-strain and controlled bale expansion for a representative alfalfa bale using the second test procedures (table 1).

Table 4. Interpolated model coefficients (eq. 5) to predict plunger restraining force during constant-strain relaxation, and measured and predicted restraining forces. Plunger force at beginning of relaxation period was 520 to 530 kN across all crops.

Test Procedure and Crop	Relaxation Duration (s)	Interpolated Relaxation Model Coefficients[a]		Plunger Force at End of Relaxation Duration (kN)		
				Measured[b]		
		k_1 ±CI	k_2 ±CI	Avg	SE	Predicted[c]
2016[d]						
Alfalfa	57	24.0 ±5.8	2.64 ±0.1	341 b	7	360 bc
Corn stover	56	32.9 ±5.6	3.87 ±0.1	402 a	3	415 a
Fescue	30	30.5 ±9.7	4.09 ±0.2	423 a	6	435 a
Switchgrass	41	24.4 ±5.0	3.91 ±0.1	403 a	3	415 ab
Wheat straw	62	46.2 ±38.3	4.11 ±0.7	318 b	42	324 c
LSD[e] (p = 0.05)				55		55
2017[f]						
Alfalfa	300	32.1 ±4.2	2.12 ±0.05	276 d	4	286 d
Corn stover	324	100 ±6.9	3.03 ±0.04	322 c	3	371 b
Fescue	251	41.3 ±5.8	2.43 ±0.06	313 c	17	321 c
Reed canarygrass	296	78.6 ±5.2	3.12 ±0.04	362 b	2	369 b
Switchgrass	297	119 ±16.3	3.72 ±0.12	370 b	3	375 b
Wheat straw	215	87.8 ±16.8	4.15 ±0.18	386 a	6	390 a
LSD[e] (p = 0.05)				11		10

[a] Model coefficients (eq. 5) determined by regression of interpolated individual bale data and 95% confidence intervals for interpolated coefficients.
[b] Measured plunger force at the end of the relaxation period before bale re-expansion.
[c] Predicted plunger force using interpolated model coefficients and equation 5.
[d] Relaxation data collected during tests using the first test procedure (table 1).
[e] Least square difference. Averages in columns with different letters are significantly different at 5% significance level.
[f] Relaxation data collected during tests using the second and third test procedures (table 1).

the same crop between 2016 and 2017. This was primarily due to differences in the duration of data collection during constant strain between years (table 4). Although the model coefficients were different between years, the predicted reductions in plunger force after a given relaxation duration were usually within ±3 percentage units.

The restraining force of the plunger as it was allowed to move during controlled bale expansion was modeled as a function of instantaneous bale density (eq. 6) using coefficients k_3 and k_4 (table 5). As the plunger was pushed by the expanding bale and bale strain was reduced, there was a rapid initial reduction in the plunger force required to restrain the bale (figs. 3 and 4). For instance, in 2016, a 6% reduction in density corresponded to an 85% reduction in plunger restraining force across all crops (table 5). This considerable reduction in restraining force with only small loss of bale density is essential to maintaining most of the recompressed bale density with restraints of reasonable tensile strength. There was an intersection point at which the total cable force equaled the plunger force, and the cables then became the main restraining mechanism (figs. 4 and 5). After the plunger was moved fully away from the bale, the bale continued to expand and lose density (fig. 5). The cable restraining force increased by an average of 128% after the plunger restraint had been removed, and the bale completed expansion (table 5). In practice, the bale would be wrapped with restraints very shortly after compression was finished, so there would be little relaxation (fig. 3). How this would

Table 5. Model coefficients k_3 and k_4 (eq. 6) used to predict plunger force as a function of instantaneous dry-basis bale density during controlled bale expansion, cable restraining force, and compressed and expanded dry-basis density of bales.

Test Procedure and Crop	Interpolated Expansion Model Coefficients[a]		Cable Restraining Force (kN)				Average Bale Density (kg m^{-3})[d]						Bale Length (cm)[e]			
			Initial[b]		Final[c]		Compressed		Partially Expanded		Fully Expanded		Compressed		Fully Expanded	
	k_3 ±CI	k_4 ±CI	Avg	SE	Avg	SE	Avg	SE	Avg	SE	Avg	SE	Avg	SE	Avg	SE
2016[f]																
Alfalfa	-	-	-	-	31.1 b	3.1	373 c	11	-	-	315 c	3	110	5	130	3
Corn stover	-	-	-	-	28.6 b	1.6	278 b	12	-	-	235 b	9	106	3	126	2
Fescue	-	-	-	-	40.4 a	1.9	286 b	5	-	-	248 b	5	120	2	139	2
Switchgrass	-	-	-	-	22.6 c	1.8	318 b	18	-	-	244 b	2	81	3	105	2
Wheat straw	-	-	-	-	30.8 b	1.2	208 a	11	-	-	185 a	7	114	6	128	5
LSD[g] (p = 0.05)					5.6		44				27					
2017[h]																
Alfalfa	-3.77 ±0.65	0.94 ±0.01	7.3 c	0.4	18.3 a	1.4	368 a	10	336 a	8	300 a	6	103	1	126	1
Corn stover	-4.71 ±0.91	0.93 ±0.02	9.5 bc	0.9	22.1 a	2.2	314 b	11	267 cd	9	242 c	6	75	2	96	1
Fescue	-5.41 ±0.72	0.92 ±0.01	9.3 bc	0.4	21.7 a	1.7	361 a	5	311 b	6	289 ab	7	84	1	105	1
Reed canarygrass	-5.68 ±0.74	0.88 ±0.03	11.6 ab	1.3	25.7 a	2.8	318 b	4	286 c	5	274 b	4	96	3	111	3
Switchgrass	-5.19 ±0.60	0.89 ±0.01	12.5 ab	1.0	25.3 a	1.8	296 c	4	264 d	3	249 c	3	94	2	111	2
Wheat straw	-4.54 ±0.26	0.89 ±0.02	14.6 a	1.3	27.1 a	2.4	238 d	7	212 e	6	202 d	7	96	1	113	1
LSD[g] (p = 0.05)			3.7		7.5		24		21		17					
2017[i]																
Corn stover	-5.01 ±1.26	0.94 ±0.04	6.4 b	0.3	16.5 a	0.7	314 b	5	288 a	6	223 c	4	76	2	107	1
Reed canarygrass	-5.69 ±0.33	0.83 ±0.01	4.6 b	0.2	12.5 b	0.8	332 a	6	300 a	5	250 a	6	89	3	119	3
Switchgrass	-7.05 ±0.81	0.43 ±0.31	8.4 a	0.7	19.0 a	1.6	293 c	2	270 b	2	235 b	6	97	1	121	4
Wheat straw	-6.87 ±0.83	0.82 ±0.03	8.3 a	0.7	16.9 a	0.9	236 d	5	221 c	6	189 d	2	95	1	119	2
LSD[g] (p = 0.05)			1.8		3.1		15		16		11					

[a] Model coefficients (eq. 6) determined by regression of interpolated individual bale data and 95% confidence intervals for interpolated coefficients.
[b] Cable restraining force at the end of controlled bale expansion when this force equaled the plunger force.
[c] Cable restraining force when plunger was free of bale and the cables were the sole means of restraint.
[d] Dry-basis bale density at maximum plunger displacement (compressed), when cable and plunger force were equal (partially expanded), and after the bale had fully expanded and was only restrained by the cables.
[e] Bale length at maximum plunger displacement (compressed) and after the bale had fully expanded. Original bale lengths were 210 cm.
[f] Data collected during tests using the first test procedure (table 1).
[g] Least square difference. Averages in columns with different letters are significantly different at 5% significance level.
[h] Data collected during tests using the second test procedures (table 1).
[i] Data collected during tests using the third test procedures (table 1).

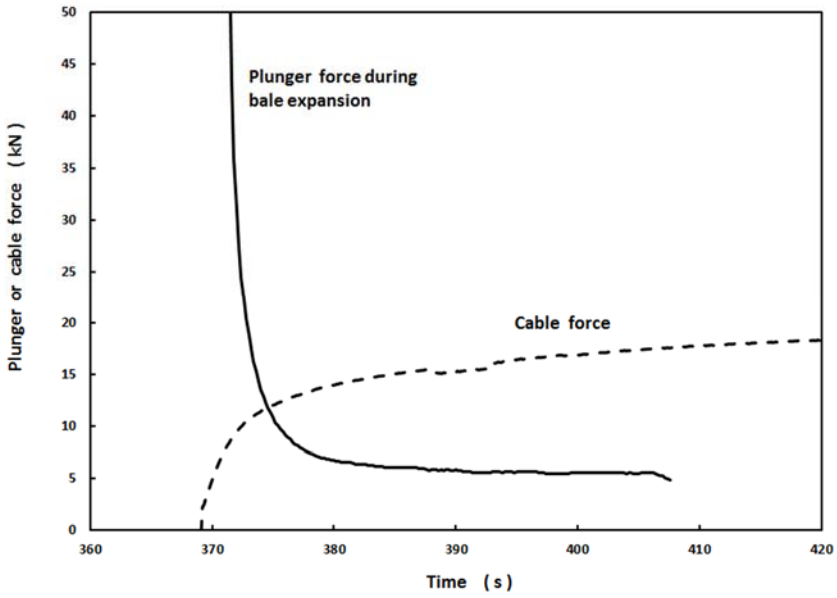

Figure 4. Plunger and restraining cable force versus time during controlled bale expansion for a representative alfalfa bale using the second test procedures (table 1).

affect the required restraining forces is unknown but should be the subject of additional research. In 2016 and 2017, the fully expanded bale densities were less than the recompressed densities by an average of 17% and 18%, respectively (table 5). After expansion into the restraints was complete and equilibrium volume was reached, the dry-basis density exceeded the target density of 205 kg m^{-3} for all crops except wheat straw.

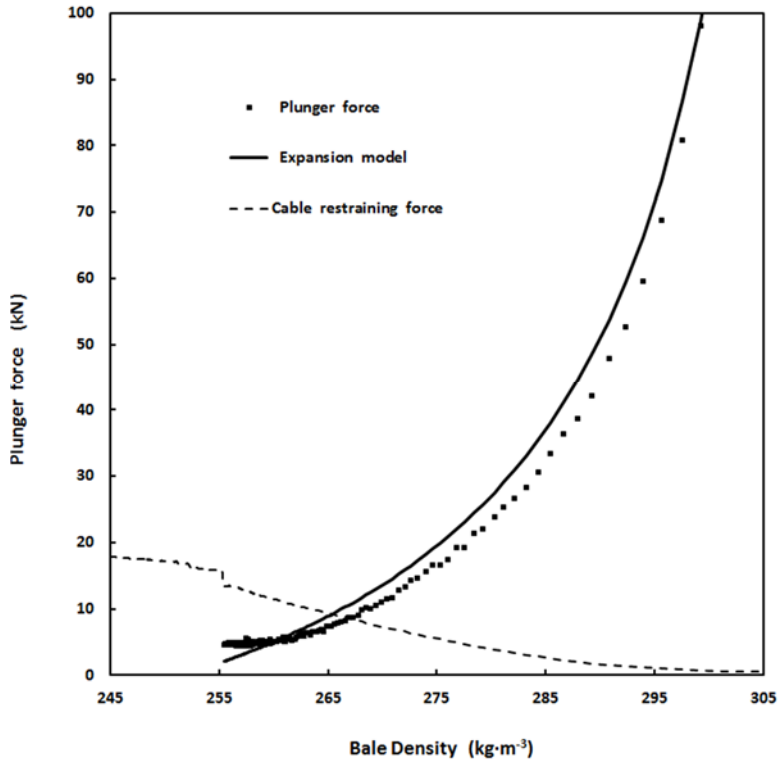

Figure 5. Plunger force versus dry-basis bale density during controlled expansion of a typical reed canarygrass bale. Because the bale was expanding and density was declining, the sequence of data occurs from right to left.

The third test procedure was used to determine the beneficial aspects of relieving some bale strain prior to applying the cable restraints. The bale was allowed to relax for approximately 5 s under constant strain, and then the plunger was retracted to produce a strain relief of approximately 10% (fig. 6). Following the strain relief, the bale continued to rebound, resulting in a slight rise in the plunger force before it reached equilibrium. This equilibrium force was typically 80% to 90% less than the maximum recompression force. The average intersection point at which the plunger and cable forces were equal was 10.8 and 6.9 kN when using the second and third test procedures, respectively, which was a 36% reduction. The average restraining force after full bale expansion was 23.4 and 16.2 kN for the second and third test procedures, respectively, which was a 31% reduction. However, relieving some bale strain to reduce the required restraining force resulted in an average reduction in fully expanded bale density of 14%.

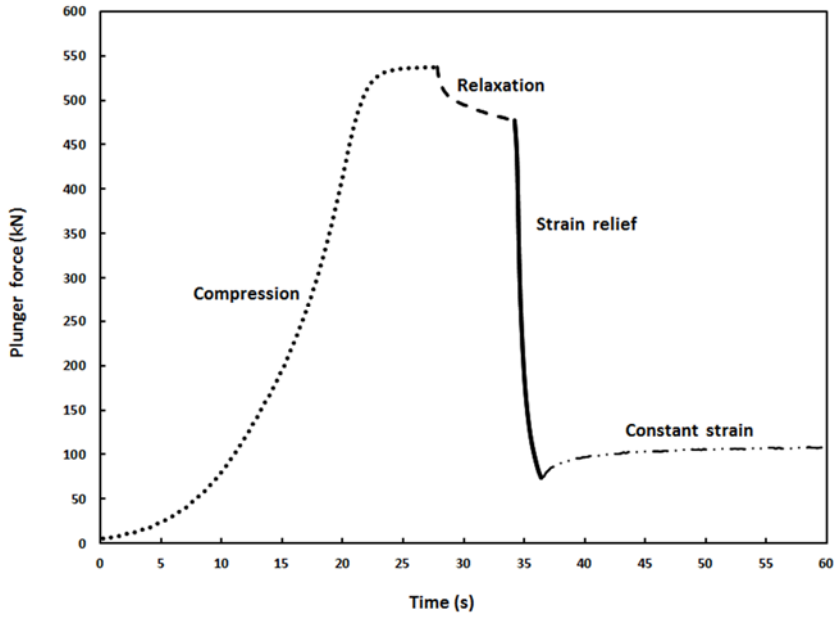

Figure 6. Plunger force versus time for a representative switchgrass bale using the third test procedure, which used 10% strain relief prior to attaching the restraining cables.

The average tension per cable after full bale expansion was approximately 2.8 and 2.0 kN when using the second and third test procedures, respectively. The maximum specified knot strength of currently available baler twine is 3.1 kN, so using conventional baler twine to restrain the recompressed bales is possible. When baling similar crops with a conventional HD LSBr, the typical maximum twine tension was between 1.2 and 1.5 kN when dry-basis density ranged from 130 to 225 kg m^{-3} (McAfee et al., 2018).

CONCLUSIONS

Recompressing LSBes approximately doubled the initial bale density when the maximum bale face pressure was 700 kPa. After relaxation and then expansion into the restraints was complete and the equilibrium volume was reached, the dry-basis LSBe density exceeded the target density of 205 kg m^{-3} for all crops except wheat straw. The specific energy for this process was considerably less than that reported to achieve similar density increases using a conventional plungerhead HD LSBr. Recompression took place in less than 30 s, which is typically less time than required to create a LSBe, so recompression and applying restraints could take place at the baler while the next bale is formed. These results suggest that creating high-density LSBes by integrating a recompressor into a LSBr is a feasible design alternative.

ACKNOWLEDGEMENTS

This research was partially sponsored by the University of Wisconsin College of Agriculture and Life Sciences and by CenUSA, a research project funded by the USDA Agriculture and Food Research Initiative (Competitive Grant No. 2011-68005-30411). We also gratefully acknowledge the financial, material, and technical support of John Deere Ottumwa Works.

REFERENCES

ASABE. (2012). S358.2: Moisture measurement- Forages. St. Joseph, MI: ASABE.

Brownell, D., & Liu, J. (2011). Field test and cost analysis of four harvesting options for herbaceous biomass handling. *Intl. J. Agric. Biol. Eng., 4*(3), 58-68.

Faborode, M. O., & O'Callaghan, J. R. (1989). A rheological model for the compaction of fibrous agricultural materials. *J. Agric. Eng. Res., 42*(3), 165-178. https://doi.org/10.1016/0021-8634(89)90048-6

Hofstetter, D. W., & Liu, J. (2011). Power requirement and energy consumption of bale compression. ASABE Paper No. 1111266. St. Joseph, MI: ASABE.

Juan, L., Xuying, L., & XueWei, B. (2010). Stress relation experiment of alfalfa bales with different cross-section. *Proc. Intl. Conf. on Mechanic Automation and Control Engineering* (pp. 3815-3817). Piscataway, NJ: IEEE. https://doi.org/10.1109/MACE.2010.5535281

Kemmerer, B., & Liu, J. (2014). Effect of harvesting time and moisture content on energy consumption of compressing switchgrass. *American J. Plant Sci., 5*(21), 3241-3249. https://doi.org/10.4236/ajps.2014.521338

Kenney, K. L., Hess, J. R., Stevens, N. A., Smith, W. A., Bonner, I. J., & Muth, D. J. (2014). Biomass logistics. In V. S. Bisaria & A. Kondo (Eds.), *Bioprocessing of renewable resources to commodity bioproducts* (pp. 29-42). Hoboken, NJ: John Wiley and Sons. https://doi.org/10.1002/9781118845394.ch2

Lacy, N. C., & Shinners, K. J. (2016). Reshaping and recompressing round biomass bales. *Trans. ASABE, 59*(4), 795-802. https://doi.org/10.13031/trans.59.11778

McAfee, J. R. (2018). Packaging and recompression of large square biomass bales. Unpublished MS thesis. Madison: University of Wisconsin.

McAfee, J. R., Shinners, K. J., & Friede, J. C. (2018). Twine tension in high-density large square bales. *Appl. Eng. Agric., 34*(3), 515-525. https://doi.org/10.13031/aea.12606

Miao, Z., Phillips, J. W., Grift, T. E., & Mathanker, S. K. (2013). Energy and pressure requirement for compression of *Miscanthus giganteus* to an extreme density. *Biosyst. Eng., 114*(1), 21-25. https://doi.org/10.1016/j.biosystemseng.2012.10.002

Mohsenin, N. N. (1970). *Physical properties of plant and animal materials.* New York, NY: Gordon and Breach.

O'Dogherty, M. J. (1989). A review of the mechanical behaviour of straw when compressed to high densities. *J. Agric. Eng. Res., 44*, 241-265. https://doi.org/10.1016/S0021-8634(89)80086-1

O'Dogherty, M. J., & Wheeler, J. A. (1984). Compression of straw to high densities in closed cylindrical dies. *J. Agric. Eng. Res., 29*(1), 61-72. https://doi.org/10.1016/0021-8634(84)90061-1

O'Dogherty, M. J., Huber, J. A., Dyson, J., & Marshall, C. J. (1995). A study of the physical and mechanical properties of wheat straw. *J. Agric. Eng. Res., 62*(2), 133-142. https://doi.org/10.1006/jaer.1995.1072

Peleg, M. (1980). Linearization of relaxation and creep curves of solid biological materials. *J. Rheol., 24*(4), 451-463. https://doi.org/10.1122/1.549567

Shah, A., & Darr, M. (2016). A techno-economic analysis of the corn stover feedstock supply system for cellulosic biorefineries. *Biofuels Bioprod. Biorefining, 10*(5), 542-559. https://doi.org/10.1002/bbb.1657

Shinners, K. J., & Friede, J. C. (2018). Energy requirements for biomass harvest and densification. *Energies, 11*(4), 780. https://doi.org/10.3390/en11040780

Shinners, K. J., Binversie, B. N., Muck, R. E., & Weimer, P. J. (2007). Comparison of wet and dry corn stover harvest and storage. *Biomass Bioenergy, 31*(4), 211-221. https://doi.org/10.1016/j.biombioe.2006.04.007

Shinners, K. J., Boettcher, G. C., Muck, R. E., Weimer, P. J., & Casler, M. D. (2010). Harvest and storage of two perennial grasses as biomass feedstocks. *Trans. ASABE, 53*(2), 359-370. https://doi.org/10.13031/2013.29566

Sokhansanj, S., Webb, E., & Turhollow, A. (2014). Cost impacts of producing high-density bales during biomass harvest. ASABE Paper No. 141912320. St. Joseph, MI: ASABE.

Steffen Systems. (2018). Bale compression systems. Salem, OR: Steffen Systems. Retrieved from http://www.steffensystems.com/bale-conversion-systems.php

Talebi, S., Tabil, L., Opoku, A., & Shaw, M. (2011). Compression and relaxation properties of timothy hay. *Intl. J. Agric. Biol. Eng., 4*(3), 69-78.

Van Pelt, T. J. (2003). Maize, soybean, and alfalfa biomass densification. *Agric. Eng. Intl.: CIGR J. Sci. Res. Devel., 5*, manuscript EE 03 002. Retrieved from http://www.cigrjournal.org/index.php/Ejounral/article/view/381/375

Wang, T., & Liu, J. (2014). Energy consumption of biomass bulk densification. ASABE Paper No. 141893416. St. Joseph, MI: ASABE.

Watts, K. C., & Bilanski, W. K. (1991). Stress relaxation of alfalfa under constant displacement. *Trans. ASAE, 34*(6), 2491-2504. https://doi.org/10.13031/2013.31897